

Spreader Pose Control Using Dual-electric Compasses

SoonShin Han
Dep. of EE.
Pusan National University.
Busan, Republic of Korea.
Ranger112@pusan.ac.kr

HeeSeok Jeong
Dep. of EE.
Pusan National University.
Busan, Republic of Korea.
heeseok@pusan.ac.kr

JangMyung Lee
Dep. of EE.
Pusan National University.
Busan, Republic of Korea.
jmlee@pusan.ac.kr

Abstract

A spreader pose control system using dual-electric compasses has been implemented by measuring the skew angle of the spreader with dual-electric compasses. In the conventional spreader pose measurement, CCD cameras, laser sensors or tilt sensors are mostly used. However those sensors are not only sensitive to the weather and disturbances but also expensive to build the system. To overcome the shortcomings, an inexpensive and efficient system to control the spreader pose has been implemented using the dual-magnetic compasses. Since the spreader iron-structures are noise sources to the magnetic compass, it is not considered to use the magnetic compass to measure the orientation of the spreader. An algorithm to eliminate the interferences of metal structures to the dual compasses has been developed in this paper. The 10:1 reduction model of a spreader control system is implemented and the control performance is demonstrated to show the effectiveness of the dual-magnetic compasses proposed in this research.

Keyword: Magnetic compass, Dual compass, Electronic compass, Spreader, Skew angle

1. Introduction

Many of hub-ports are trying to develop a fully automated loading/unloading system to escape from the heavy human work loads. Main technologies for the successful management of the automated port are the automated loading/unloading using cranes and the automated navigation of carrying vehicles.

Especially the loading/unloading time is a crucial factor for the ship staying at a port. The two types of containers, 20 ft and 40 ft, are handled by the specialized equipment. Main equipments are a container crane and a yard crane. The container crane speed is one of the most important in determining the container processing capability of a port. The yard crane is carrying the containers to stock and to load on the carrying vehicle. Both of these two cranes have the same structures of a horizontal-motion trolley and a vertical-motion spreader, and carry the containers to a desired location.

To load or unload the containers precisely, the pose control of the spreader is essential with the precise measurement of the skew and sway angles. The precise

pose measurement reduces the monitoring operator's care about the unmanned crane in the automated port[1]. For the spreader pose measurement, CCD cameras, lasers, and tilt sensors mainly have been utilized in the most operating automated ports[2-4]. However, there are some limitations in using the conventional sensors for the measurement of spreader pose. The CCD cameras require the image processing procedures which take a lot of time, and the images are very sensitive to weather conditions. The laser sensors are very expensive and have the dead angle in measuring skew angles.

In this paper, the spreader orientation is measured and controlled by using the dual electric compasses which are robust against the iron structures. In general, the compass is very sensitive to the iron structures, and it cannot be used near at the iron structure. Using the dual electric compasses, the sensitiveness to the iron structures has been eliminated and also the disturbances from the neighboring objects have been filtered out[5,6] to achieve the skew angle control. Section 2 introduces the conventional usage of the electric compass. In section 3, the principle of the dual-electric compasses proposed in this paper have been described. Section 4 analyzes the experimental results, and section 5 concludes this paper and indicates future works on this topic.

2. Single Compass Compensation

There are three basic compensations required for the compass: zero-offset, output sensitivity variation, and non-orthogonal error. The error compensation techniques are explained for the general single compass.

2.1 Zero-offset

The output offset of the compass comes from the device itself and from the amplifier. The offset depends on the sensor tolerance and temperature, and the offset value is obtained as

$$V_{offset} = (V_{x,y \max} - V_{x,y \min}) / 2 \quad (1)$$

where V_{offset} is zero when there is neither disturbance nor device-offset.

Using the offset value, the output is corrected as

$$V_{x,y \text{ corrected}} = V_{x,y \text{ output}} - V_{offset} \cdot \quad (2)$$

2.2 Output sensitivity variation

The two sensors for x- and y-axis may have different sensitivity to magnetism and amplification factors. The errors can be compensated by using scale factors. That is, when the scale factor for x-axes is represented as, $S_{V_x} = 1$, then the scale factor for y-axes, S_{V_y} can be represented as

$$S_{V_y} = \frac{V_{y \max} - V_{y \min}}{V_{x \max} - V_{x \min}}. \quad (3)$$

Using the scale factor for y-axes, S_{V_y} , the outputs along x- and y-axis are matched to represent the azimuth angle correctly.

2.3 Non-orthogonal error

In the manufacturing process of the sensor, the non-orthogonal error of up to 2° exists. The error can be represented as

$$V_y = V_{\max} \cdot \sin(\alpha + \beta) \quad (4a)$$

$$V_x = V_{\max} \cdot \cos \alpha. \quad (4b)$$

From Eq's. (4a) and (4b), α and β can be obtained. Therefore the corrected y-axis output can be obtained as

$$V_{y \text{ corrected}} = \frac{V_y}{\cos \beta} - V_x \cdot \tan \beta. \quad (5)$$

3. Dual Compass Compensation

The compass is very sensitive to the interferences from magnetic materials. To resolve this shortcoming, in this approach, dual compasses arranged in 180° phase difference have been utilized as shown in Fig. 1.

3.1 Output phase error

The interference from the metal-structures to the two sensors in 180° phase difference can be modeled and compared with the earth magnetism in Fig. 1.

The spread magnetism represents the magnetism of the iron structures which are magnetized by the earth magnetism. The interference results in the addition to one sensor and the subtraction to the other 180° phase difference sensor with the earth magnetism. If there exists only the pure earth magnetism, the addition of the two x- and y-axis outputs of the two compasses is zero.

However by the effects of the interference, the summation is not zero in the metal-structures normally. This compensation algorithm for this interference has been developed in this paper and will be described in detail in the following subsection.

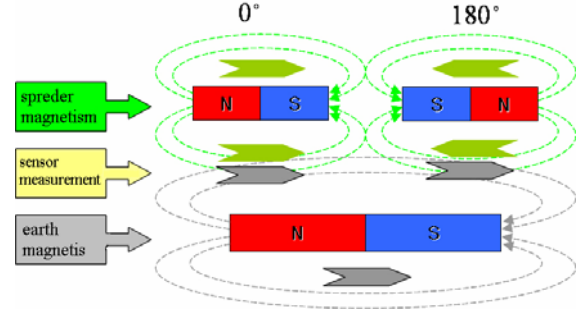


Fig. 1. Relation between earth magnetism and the interference.

3.2 Output amplitude compensation

The outputs of the dual compasses are recorded on the metal-structure to be used while the structure is rotated by 360° , the results are represented as two circles in Fig. 2. To remove out the interference effects, the two circles are properly shifted to the center and to match the radii of the circles to the same.

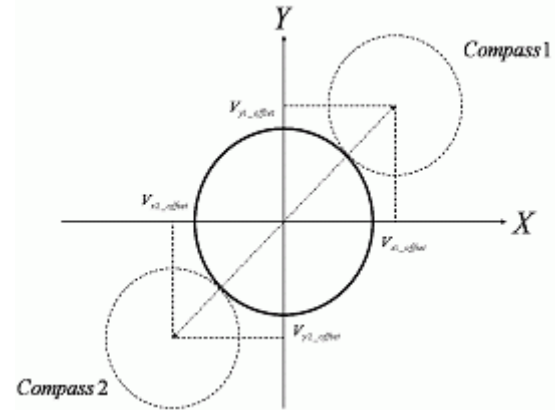


Fig. 2. Change of magnetized circles with metal-structures.

Through this compensation process, the interference from the metal-structure is pre-specified and the results can be utilized for the real-time interference compensation.

The normalization process for the two compass outputs starts with the measured offset value as follows:

$$V_{1r} = \left| V_{1\max} - V_{1\text{offset}} \right| \quad (6a)$$

$$V_{2r} = \left| V_{2\max} - V_{2\text{offset}} \right| \quad (6b)$$

where $V_{1\max}$ and $V_{2\max}$ are the maximum values obtained from Fig. 2, $V_{1\text{offset}} = \sqrt{V_{1x,\text{offset}}^2 + V_{1y,\text{offset}}^2}$ and $V_{2\text{offset}} = \sqrt{V_{2x,\text{offset}}^2 + V_{2y,\text{offset}}^2}$. Now the scale factor for the sensor 2 can be defined, assuming $V_{1sf} = 1$ as follows:

$$V_{2sf} = \frac{V_{1r}}{V_{2r}}. \quad (7)$$

Therefore the normalized x-directional output can be obtained as

$$V_{x1\ corrected} = V_{x1} - V_{x1, offset} \quad (8a)$$

$$V_{x2\ corrected} = (V_{x2} - V_{x2, offset}) \cdot V_{2sf}. \quad (8b)$$

Note that the y-directional output can be also obtained by replacing x as y in equations (8a) and (8b).

Through the process, the magnetized circle can be moved to the origin of the measuring coordinates.

3.3 Disturbance compensation

The interference from the neighboring structures cannot be filtered out on the real time with only a single compass. In this approach, using the dual compasses, the interference is eliminated.

To implement a stable skew angle measuring system using the dual compasses, here the rejection of dynamic disturbances using the dual-compasses has been proposed. By the Eq. (8), the two magnetized circles are normalized, and the two circles may have exactly same outputs when there is no disturbance. When there exists disturbing magnetism, the rotation of θ does not result in the same variations in both compasses. Instead, the compasses have the azimuth angles of ρ and σ which do not have 180° phase difference but have ε error.

The x and y directional error components can be obtained from the outputs of the dual compasses, respectively, as

$$error_x = \frac{V_{x1} + V_{x2}}{2} \quad (9a)$$

$$error_y = \frac{V_{y1} + V_{y2}}{2} \quad (9b)$$

where V_{x1}, V_{x2}, V_{y1} and V_{y2} are x and y directional outputs of sensors 1 and 2, respectively. The magnetized circle can be described by the radius and phase as follows:

$$R = \sqrt{V_x^2 + V_y^2} \quad (10a)$$

$$\theta = \tan^{-1} \frac{V_y}{V_x}. \quad (10b)$$

Since the radius is not constant by the disturbance, the shape of the magnetized circles becomes ellipsoid with this disturbance.

4. Experiments and Results

In this section, the constitution of the experimental equipment has been illustrated, which measures and controls the skew angle of the 10:1 reduction model spreader. The dual compasses are utilized for the angle measurements and the control results show that the

control accuracy with the dual compasses is high enough to be used for the spreader pose control within the flipper error tolerance.

4.1 Experimental environment

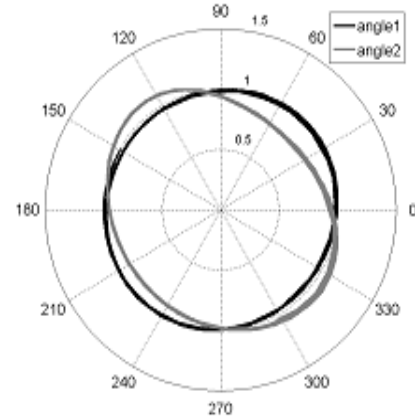
Since there were some difficulties in feeding the control cables on the center of the model spreader, the compasses are installed at each end of the spreader symmetrically. By the experiment 1, the compasses become ready to be used by compensating all the offsets. In the experiment 2, the structural inference is added by putting the two compasses on the metal-frame.

For the calibration process, a motor is installed at the bottom of the spread and its angle is controlled according to the encoder value.

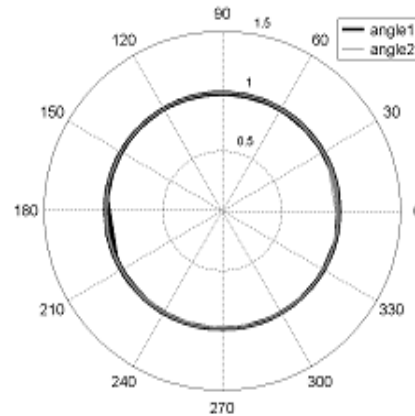
4.2 Error compensation

By the first experiment, the magnetized circles before and after compensation have been drawn in Fig. 3(a) and Fig. 3(b), respectively.

The magnetic field intensity has been increased at a compass while for the other has been decreased. Also the interference is not constant so that the magnetized circles become ellipsoids as expected.



(a). Before interference compensation.



(b). After interference compensation

Fig. 3. Dual compass output.

4.3 Skew angle measurement

The spreaders of the crane operating in the harbors can be rotated about $\pm 15^\circ$ during the loading and unloading operations. And the allowable angle error for both of 20 ft and 40 ft containers are 1° for the normal loading/unloading operations. Therefore for the fully automated crane, the skew angle error should be kept within 1° by the control system.

Using the single compass, the skew angle of the spreader which is rotated $\pm 15^\circ$ has been measured and recorded in Fig. 4.

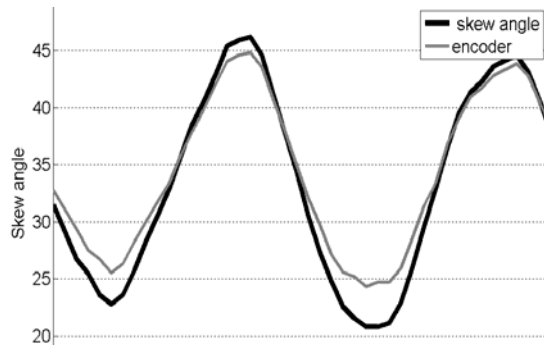


Fig. 4. Experiments of measuring of skew angle.

Notice that for the error measurement, the high precision encoder data have been used as the reference values. As it is illustrated in Fig. 4, the skew angle measurement by the single compass has the maximum 4° error which is out of the allowable angle error for the flipper. There is no effective scheme to reduce this error so far.

When the dual compasses have been used for the skew angle measurements, there was nearly recognizable error in Fig. 5. With the dual compasses, the maximum measurement error for the skew angle is less than 0.5° . Therefore it is precise enough to be utilized to control the pose of the spreader as a skew angle sensor.

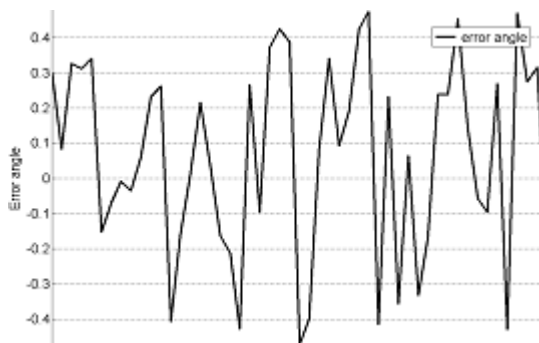


Fig. 5. Experiment of skew angle.

5. Conclusions

The spreader pose control system has been implemented by using the dual-electric compasses which are robust against both the structural interference and

dynamic disturbances. The skew angle control is the most difficult problem in the control of the spreader for the loading/unloading operations since there is not any suitable sensor for the measurement of the skew angle. With the development of the dual-electric compasses, the automated crane can be robust against the weather conditions and be a precise and economical system. In the compensation processes, there were magnetic hysteresis which can be modeled and eliminated to improve the accuracy as a future research.

Acknowledgment

This work was supported by the Regional Research Centers Program (Research Center for Logistics Information Technology), granted by the Korean Ministry of Education & Human Resources Development.

References

- [1] Kanji Obata, Koji Uchida, Takashi Chikura, Hirofumi Yoshikawa and Tadaaki Monzen, "Automated Transfer Crane," *Mitsubishi Heavy Industries Technical Review*, Vol. 40, no. 2, pp. 1 ~ 5, Jan. 2003.
- [2] John R. Holmquist, "Laser Guided Loading System," *IEEE Trans. Industry Applications*, Vol. 38, no. 3, pp. 752~757, May, 2002.
- [3] Kyung-Moon Lee, Yang-Hwan Kim, Jae-Mu Yun and Jang-Myung Lee, "Magnetic-interference-free dual-electric compass," *Sensors and Actuators*, A120, pp. 441~450, Jan. 2005.
- [4] J. Ko, W. Kang, Y. H. Kim and Jang-Myung Lee, "Robust Electric Compass to Dynamic Magnetic Field Interference," *Journal of Control, Automation, and Systems Engineering*, Vol.11, no. 1, pp. 27~33, Jan. 2005.
- [5] Lenz, J.E, "A review of magnetic sensors," *Proceedings of the IEEE*, Vol. 78, Issue 6, pp. 973~989, Jun. 1990.
- [6] Racz. R, Schott. C and Huber. S, "Electronic compass sensor," *Sensors, Proceedings of IEEE*, Vol. 3, pp. 1446 ~ 1449, Oct. 2004.